ORGANIC LETTERS

2000
Vol. 2, No. 13
1927−1929

Mechanistic Insights into the Factors Determining *Exo–Endo* Selectivity in the Lewis Acid-Catalyzed Diels–Alder Reaction of 1,3-Dienes with 2-Cycloalkenones

Min Ge, Brian M. Stoltz, and E. J. Corey*

Department of Chemistry and Chemical Biology Harvard University, 12 Oxford Street, Cambridge, Massachusetts 02138

corey@chemistry.harvard.edu

Received May 1, 2000

ABSTRACT

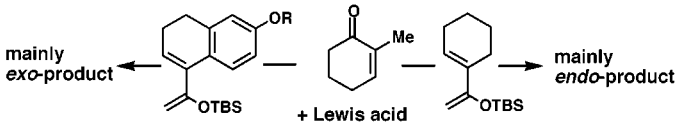

We adduce evidence that the asynchronous, Lewis acid-catalyzed Diels–Alder reaction of 2-cycloalkenones with nonsimple α,β-enones can proceed via transition states in which the 1,3-diene subunit is skewed, i.e., nonplanar, with profound effects on the ratio of *exo* and *endo* addition products.

During the course of research on the total synthesis of nicandrenone, one of us (B.M.S.) discovered an interesting *exo*-selective, Lewis acid-catalyzed Diels−Alder reaction of 2-methyl-2-cyclohexenone (**1**) and diene **2** to form *exo* adduct **3** as the principal product (TBS = *tert*-butyldimethylsilyl,

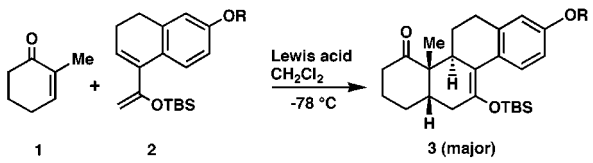

R = allyl).[1] Despite the great potential of such powerful constructions in synthesis, this area of synthetic methodology remains largely unexploited. For this reason we embarked on the research described herein on the study of factors influencing *exo*−*endo* product selectivity and the mechanistic pathways of Lewis acid-catalyzed Diels−Alder reactions of 2-cycloalkenones. It was hoped that this work would set the stage for development of catalytic enantioselective versions of this process which might achieve success approaching that already attained, for example, with dienes and α,β-enals.[2,3]

The first task that we undertook was exploration of the source of *exo* selectivity (up to 8:1) in the formation of **3** from **1** and **2** in sharp contrast to the known $AlCl_3$-catalyzed reactions of 2-cyclohexenone or 2-methyl-2-cyclohexenone and cyclopentadiene which afford mainly the *endo* adducts (9:1 and 20:1 at 40 °C, respectively).[3,4] Toward this end we chose first to simplify the diene component from **2** to **4**. This modest change of diene structure resulted in the preferred formation of *endo* adduct **5** from 2-methyl-2-cyclohexenone

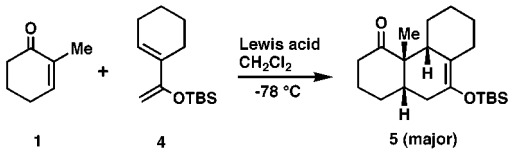

with $SnBr_4$ as catalyst (*endo*:*exo* 7.3:1 at −78 °C). The structure of the major Diels−Alder adduct **5** was determined by X-ray crystallographic analysis of the crystalline trans-

(1) Stoltz, B. M.; Corey, E. J. Unpublished.

10.1021/ol0060026 CCC: $19.00
Published on Web 05/27/2000

formation product, tosylhydrazone **9**, which was synthesized as outlined in Scheme 1. Reduction of a mixture of the *endo*

Scheme 1

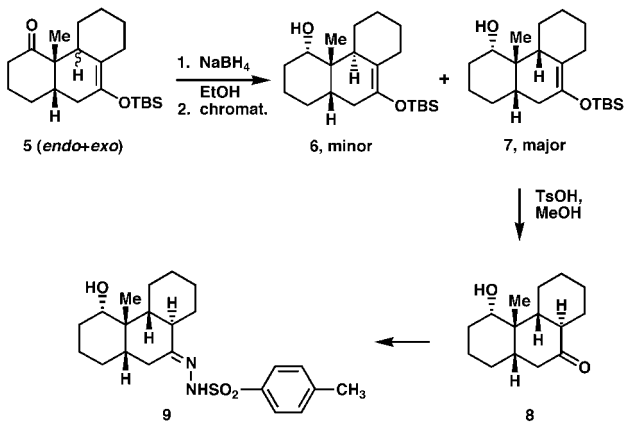

and *exo* diastereomers of **5** with sodium borohydride in ethanol at 0 °C gave the corresponding axial OH reduction products (**6** and **7**, TLC R_f values on silica gel plates 0.15 and 0.43 with 9:1 hexanes−EtOAc) which were readily separated by column chromatography on silica gel. Desilylation of the major *endo* alcohol **7** using 0.1% tosic acid in methanol at 23 °C for 3 h produced keto alcohol **8** which upon reaction with *p*-toluenesulfonylhydrazine in 96:4 ethanol−acetic acid at 70 °C for 1 h afforded crystalline *p*-toluenesulfonylhydrazone **9**, mp 176 °C (dec). The structure determined for **9** by X-ray crystallography is shown in Figure 1.[5]

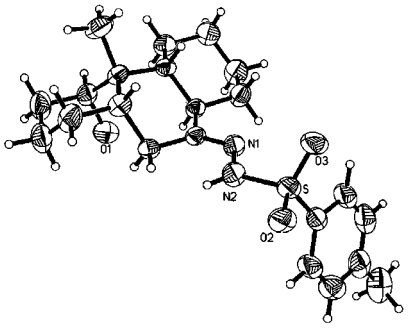

Figure 1. ORTEP structure for tosylhydrazone **9**.

The *endo* preference for the Diels−Alder reaction of **1** and **4** to give **5** is an intrinsic one which does not depend on the choice of Lewis acid. The results of experiments on this addition reaction with nine different Lewis acids, summarized in Table 1, reveal in each case a marked preference for *endo* adduct formation. The use of bulky Lewis acids, which might have been expected to disfavor the *endo* addition in a transition state with [4 + 2]-cycloaddition-like geometry, if anything, seems to enhance the *endo* pathway (see Bu_3SnOTf and $SbCl_5$ entries in Table 1).

Table 1.

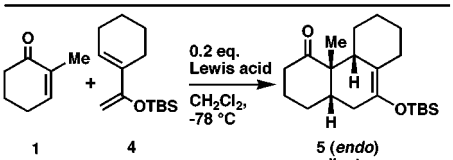

Lewis Acid	yield, %	*endo*/*exo*	time (h)
$SnBr_4$	94	7.3	<0.3
$SnCl_4$	84	3.6	<0.3
Bu_3SnOTf[a]	58	11.5	14
$Bu_2Sn(OTf)_2$	81	8.1	4
$Bu_2Sn(OSO_2C_4F_9)_2$	94	9	0.5
$MeAlCl_2$	91	6.8	<0.3
$SbCl_5$	90	10.5	<0.3
$B(C_6F_5)_3$	62	7.0	2
$In(OTf)_3$	73	7.5	<0.3

[a] -60 °C

At first glance it may seem paradoxical that monocyclic diene **4** resembles cyclopentadiene in that both show an *endo* preference in the Diels−Alder reaction with 2-methyl-2-cyclohexenone, in contrast to the structurally related bicyclic diene **2** which reacts to form mainly the *exo* adduct.[6] However, a detailed examination of possible transition state structures for the reactions **1** + **4** → **5** and **1** + **2** → **3** reveals a logical reason for the observed *exo/endo* preferences which is related to the conformational energetics of dienes **2** and **4**. Molecular mechanics (MM2) calculations for simple analogues of **2** and **4**, **2′** and **4′**, are summarized in Table 2. For clarity of comparison, the vinyl methyl ether subunits of **2′** and **4′** were fixed in the coplanar geometry shown, i.e.:

From the data in Table 2, it is clear that the planar diene conformers **4′**, $\phi = 0°$, and **4′**, $\phi = 180°$, are close in energy to the global minimum. Thus, as with cyclopentadiene, the planar conformer **4**, $\phi = 0°$, can lead to a correspondingly low energy transition state structure, free of appreciable steric

(2) For recent reviews, see: (a) Diaz, L. D. *J. Braz. Chem. Soc.* **1997**, *8*, 289. (b) Pindur, U.; Lutz, G.; Otto, C. *Chem. Rev.* **1993**, *93*, 741. (c) Corey, E. J.; Guzman-Perez, A. *Angew. Chem., Int. Ed.* **1998**, *37*, 388. (d) Corey, E. J.; Rohde, J. J. *Tetrahedron Lett.* **1997**, *38*, 37. (e) Corey, E. J.; Barnes-Seeman, D.; Lee, T. W. *Tetrahedron Lett.* **1997**, *38*, 1699.

(3) (a) Angell, E. C.; Fringuelli, F.; Guo, M.; Minuti, L.; Taticchi, A.; Wenkert, E. *J. Org. Chem.* **1988**, *53*, 4325. (b) Angell, E. C.; Fringuelli, F.; Minuti, L.; Pizzo, F.; Porter, B.; Taticchi, A.; Wenkert, E. *J. Org. Chem.* **1986**, *51*, 2649.

(4) See also: Das, J.; Kakushima, M.; Valenta, Z.; Jankowski, K.; Luce, R. *Can. J. Chem.* **1984**, *62*, 411.

(5) Detailed X-ray crystallographic data are available from the Cambridge Crystallographic Data Center, 12 Union Road, Cambridge CB2 1EZ, U.K.

Table 2. Energy (kcal/mol) as a Function of 2,3-Dihedral Angle for the 1,3-Dienes **2′** and **4′**

2,3-dihedral angle, ϕ °	E (kcal/mol) 4′, ϕ = 0°	2′, ϕ = 0°
0	10.8	16.2
15	10.7	14
30	10.8	12.1
45	11.9	11.3
90	16.7	13.4
135	13.8	12.9
165	12.4	21.7
180	11.6	33.4

repulsion in the diene part. In contrast, however, bicyclic diene **2′** is strongly destabilized in planar conformer **2′**, $\phi = 0°$ (and even more so in **2′**, $\phi = 180°$), by repulsions involving the aromatic ring and the 1,3-diene substituents.[7] This leads to the expectation that the transition state for the reaction of the enone **1**−Lewis acid complex with **2′** (or **2**) will be of minimum energy, not with $\phi = 0°$ but more likely $\phi = 15-30°$. This moderate twist from planarity largely alleviates steric repulsions in the diene part while preserving most of the charge π-delocalization over the 1,3-diene, which is diminished by the factor cos ϕ (only 0.96 for $\phi = 15°$ and 0.87 for $\phi = 30°$). It is also clear that the transition state for these Diels−Alder reactions will be highly unsymmetrical in the sense that by far the stronger new bond will be between the β-carbon of the enone−Lewis acid complex and the terminal methylene group of the diene.[8] Given these structural parameters for the transition state $[\mathbf{1} + \mathbf{2}]^{\neq}$, a simple explanation emerges for the preference of the *exo* over the *endo* pathway. In the *endo*-$[\mathbf{1} + \mathbf{2}]$ transition state with $\phi = 15-30°$, there is a repulsive steric interaction between the enone part and the benzenoid ring of **2** which is absent or considerably smaller in the corresponding *exo*-$[\mathbf{1} + \mathbf{2}]$ transition state as depicted in Figure 2 (Lewis acid deleted). In particular, because of the nonplanarity of the 1,3-diene, the mean planes of the α,β-enone component and the dihydronaphthalene subunit are canted so as to bring the methylenes of the former into repulsive contact with the aromatic ring in the transition state for *endo* addition.

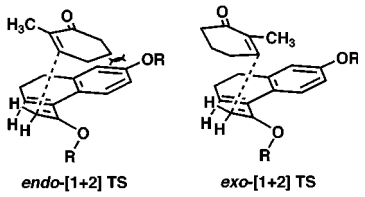

Figure 2.

Although the ring planes are also canted in the *exo* transition state structure shown in Figure 2, there do not seem to be significant repulsions involving the aromatic ring and the α,β-enone.

Accordingly, the aromatic ring of diene **2** exerts dual effects on the *endo*−*exo* ratio in Diels−Alder addition, the first associated with steric repulsions which favor the skewed diene geometry in the transition state and the second involving direct repulsion with the methylene portion of the dienophile. The nonaromatic, monocyclic diene **4** is thus fundamentally more like 1,3-cyclopentadiene than its analogue diene **2**, because it lacks the crucial aromatic ring and associated steric effects.

The studies reported herein have produced new insights into the Lewis acid-catalyzed Diels−Alder reactions of α,β-enones with nonsimple dienes which provide not only a better theoretical understanding of these fundamentally important chemical transformations but also a valuable calibration for synthetic planning and design.

The experimental procedure for the synthesis of **5** from **1** and **4** is detailed in ref 9.

Acknowledgment. This research was assisted financially by a grant from the National Institutes of Health.

OL0060026

(6) The assignment of structure **3** to the major (*exo*) adduct from **1** and **2** was also determined unambiguously by X-ray crystallographic analysis (unpublished results of Brian M. Stoltz).

(7) ^{1}H NMR NOE measurements with diene **2** (R = allyl) confirmed the nonplanarity of the 1,3-diene moiety, since the terminal olefinic methylene proton which is trans to the OTBS group showed positive NOE enhancement with both the olefinic proton at the other end of the diene (+2.2%) and the peri proton on the benzenoid ring (+2.7%).

(8) (a) Singleton, D. A.; Merrigan, S. R.; Beno, B. R.; Houk, K. N. *Tetrahedron Lett.* **1999**, *40*, 5817. (b) Garcia, J. I.; Martinez-Merino, V.; Mayoral, J. A.; Salvatella, L. *J. Am. Chem. Soc.* **1998**, *120*, 2415.

(9) To a solution of CH_2Cl_2 (1.1 mL), toluene (3.3 mL), and 2-methyl 2-cyclohexenone (100 μL, 0.9 mmol, 90% pure) in a flame-dried flask at −78 °C was added $SnCl_4$ (180 μL of 1 M solution in CH_2Cl_2, 0.180 mmol). TBS diene **4** (260 μL, 0.988 mmol) was then added dropwise through a 22 gauge needle. TLC analysis indicated complete reaction within 30 min. The reaction mixture was treated with 100 μL of Et_3N and 10 mL of aqueous $NaHCO_3$ solution, allowed to warm to room temperature, and diluted with 10 mL of aqueous KNa tartrate. The mixture was extracted with CH_2Cl_2 (3 × 10 mL). The CH_2Cl_2 extracts were dried over anhydrous Na_2SO_4 and concentrated to give an oil which was purified by flash chromatography (6% EtOAc−hexane) to give 236.7 mg (84.2%) of adducts **5** as a 4:1 mixture of *endo* and *exo* isomers. The pure isomers can be obtained by reducing the mixture to the corresponding alcohols **6** and **7** ($NaBH_4$, EtOH, 0 °C) which then were separated by column chromatography on silica gel and oxidized at 0 °C in CH_2Cl_2 with the Dess−Martin periodinane reagent to give pure *endo*-**5** and *exo*-**5**. *endo*-**5**: R_f 0.45 (10% EtOAc/hexane); FTIR (film) 1254, 1699, 2856, 2930 cm^{-1}; ^{1}H NMR ($CDCl_3$, 400 MHz) δ 2.96−2.90 (dd, J = 10.2, 3.0 Hz, 1H), 2.58−2.48 (dt, J = 16.8, 4.4 Hz, 1H), 2.42−2.33 (m, 1H), 2.30−2.20 (m, 1H), 2.0−1.4 (m, 13H), 1.3−1.18 (m, 4H), 0.98 (s, 9H), 0.10 (s, 6H) ppm; ^{13}C NMR ($CDCl_3$, 100 MHz) δ 215.7, 137.9, 115.8, 50.7, 47.0, 42.2, 41.2, 33.9, 33.8, 28.3, 28.2, 27.8, 27.3, 26.3, 24.9, 23.8, 18.7, −3.3, −3.4 ppm; mp 100−101 °C; HRMS (EI$^+$) *m*/*z* calcd for $[C_{21}H_{36}O_2Si]^+$ (M^+) 348.2485, found 348.2472; *exo*-**5**: R_f 0.45 (10% EtOAc/hexane); FTIR (film) 1365, 1704, 2858, 2898 cm^{-1}; ^{1}H NMR ($CDCl_3$, 400 MHz) δ 3.0−2.9 (m, 1H), 2.75−2.6 (m, 1H), 2.5−2.35 (m, 2H), 2.27−2.20 (m, 1H), 2.10−2.0 (m, 1H), 1.90−1.50 (m, 7H), 1.50−1.42 (m, 1H), 1.32−1.00 (m, 7H), 0.95 (s, 9H), 0.12 (s, 6H) ppm; ^{13}C NMR ($CDCl_3$, 100 MHz) δ 215.3, 139.4, 114.0, 51.7, 44.6, 40.0, 37.8, 33.9, 27.8, 27.5, 26.6, 26.32, 26.30, 26.2, 26.1, 18.7, 17.1, −3.3, −3.5 ppm; mp 58−59 °C.